Journal of Dental Sciences 21 (2026) 475–483

Available online at www.sciencedirect.com

ScienceDirect

journal homepage: www.e-jds.com

Original Article

Tumor microenvironment-derived IL-32 promotes aggressive phenotypes and stem cell traits in head and neck squamous cell carcinoma

Nien-Tzu Liu [a,b], Shin-Hsien Yang [a,c], Yi-Ming Chang [d,e], Jian-Hong Yu [f,g], Su-Feng Chen [g], Yaoh-Shiang Lin [h], Yu-Chun Lin [a,b,d*]

[a] *Graduate Institute of Medical Sciences, National Defense Medical University, Taipei, Taiwan*
[b] *Department of Pathology, National Defense Medical University & Tri-Service General Hospital, Taipei, Taiwan*
[c] *Office of General Affairs and Occupational Safety and Health, National Defense Medical University, Taipei, Taiwan*
[d] *Institute of Pathology and Parasitology, National Defense Medical University, Taipei, Taiwan*
[e] *Department of Pathology and Laboratory Medicine, Kaohsiung Veterans General Hospital, Kaohsiung, Taiwan*
[f] *Orthodontics, Department of Dentistry, China Medical University Hospital, Taichung, Taiwan*
[g] *School of Dentistry, College of Dentistry, China Medical University, Taichung, Taiwan*
[h] *Department of Otorhinolaryngology, Kaohsiung Veterans General Hospital, Kaohsiung, Taiwan*

Received 6 August 2025; Final revision received 8 October 2025
Available online 6 November 2025

KEYWORDS
Head and neck squamous cell carcinoma;
Cancer-associated fibroblasts;
Interleukin-32;
Epithelial–mesenchymal

Abstract *Background/purpose:* Head and neck squamous cell carcinoma (HNSCC) is an aggressive malignancy distinguished by marked invasiveness, a high metastatic propensity, and poor prognosis. Cancer-associated fibroblasts (CAFs) within the tumour microenvironment secrete numerous mediators that accelerate tumour progression; however, the precise contribution of CAF-derived interleukin-32 (IL-32) remains unclear. This study examined the influence of CAF-derived IL-32 on invasion, epithelial–mesenchymal transition (EMT), and cancer-stem-cell (CSC) traits in HNSCC.

Materials and methods: Primary CAFs and normal fibroblasts (NFs) were isolated from HNSCC specimens. IL-32 expression was quantified by microarray analysis, quantitative PCR, Western blotting, and enzyme-linked immunosorbent assay. Migration and invasion of FaDu and

* Corresponding author. Department of Pathology, National Defense Medical University & Tri-Service General Hospital, No. 325, Sec.2, Chenggong Rd., Neihu District, Taipei City 114202, Taiwan.
E-mail address: yuchunlin@mail.ndmctsgh.edu.tw (Y.-C. Lin).

https://doi.org/10.1016/j.jds.2025.10.010

transition;
Cancer stem cells

SCC25 cells were assessed with Transwell assays after exposure to CAF-conditioned medium or recombinant IL-32. EMT markers were evaluated by Western blotting, whereas sphere-formation assays and flow cytometry for $CD133^+/CD44^+/CD24^+$ populations were used to determine stemness.

Results: IL-32 was significantly up-regulated in CAFs compared with NFs. Both CAF-conditioned medium and recombinant IL-32 markedly increased the migratory and invasive capacities of HNSCC cells. These treatments reduced E-cadherin and increased Vimentin, Snail, and Twist expression, while enhancing sphere formation and expanding $CD24^+$, $CD44^+$ and $CD133^+$ sub-populations.

Conclusion: CAFs promote HNSCC progression through IL-32-mediated enhancement of invasion, EMT induction, and CSC properties. Targeting IL-32 signalling may represent a promising therapeutic approach to improve outcomes in HNSCC.

Introduction

Head and neck squamous cell carcinoma (HNSCC) represents a considerable global health burden,[1] with more than 600 000 new diagnoses each year,[2,3] particularly in regions where tobacco, alcohol, and betel-nut consumption are prevalent.[4] Despite advances in surgery, radiotherapy, and chemotherapy, the five-year survival rate remains dismal owing to frequent locoregional recurrence and distant metastasis.[5] These clinical shortcomings are driven not only by intrinsic genetic alterations but also by the complex influence of the tumour micro-environment (TME).[6]

The TME comprises stromal cells, immune infiltrates, and extracellular-matrix components that collectively regulate tumour growth, invasion, and treatment response.[7] Persistent inflammation mediated by cytokines such as interleukin (IL)-1β, IL-6,[8] and tumour necrosis factor-α (TNF-α) fosters genomic instability, angiogenesis, and matrix remodelling, thereby facilitating malignant dissemination. Elucidating these multifaceted interactions is essential for identifying therapeutic targets capable of disrupting stromal support for tumour progression.[9,10]

Among stromal constituents, cancer-associated fibroblasts (CAFs) are pivotal.[11] Characterised by activation markers including α-smooth-muscle actin and vimentin, CAFs secrete cytokines (e.g., IL-6, IL-8, and stromal-derived factor-1) alongside extracellular-matrix proteins that enhance epithelial—mesenchymal transition (EMT), invasion, and metastatic potential.[12] Increased CAF density in HNSCC specimens is consistently associated with an unfavourable prognosis.[13] Emerging evidence indicates that interleukin-32 (IL-32) a pro-inflammatory cytokine abundantly expressed by CAFs-may also drive aggressive tumour behaviour;[14,15] nevertheless, its precise role in HNSCC remains poorly defined.

Originally described for its immunomodulatory functions, IL-32 activates oncogenic pathways such as nuclear factor-κB and signal transducer and activator of transcription 3, both implicated in tumour invasiveness and therapeutic resistance.[16,17] However, the mechanistic link between CAF-derived IL-32 and HNSCC malignancy has not yet been delineated. Accordingly, we sought to determine whether CAF-derived interleukin-32 (IL-32) contributes to invasion, epithelial—mesenchymal transition, and cancer-stem-cell traits in HNSCC, to inform future stromal-targeted approaches.

Materials and methods

Patient specimens and fibroblast isolation

Fresh HNSCC tumours and adjacent macroscopically normal mucosa were obtained from patients undergoing resection at Kaohsiung Veterans General Hospital, Taiwan (IRB no. KSVGH20-CT4-19). Tissues were finely minced, digested in DMEM/F12 containing 1 mg mL^{-1} type I collagenase, filtered through a 70 μm nylon mesh, and pelleted at 300 g for 10 min. Cells were cultured in DMEM/F12 supplemented with 10 % (v/v) fetal bovine serum (FBS). Spindle-shaped fibroblast colonies emerged within two weeks; cancer-associated fibroblasts (CAFs) and normal fibroblasts (NFs) were distinguished morphologically and confirmed by immunocytochemistry for α-smooth-muscle actin and vimentin. Passages 3—6 were used in all experiments.

HNSCC cell lines and culture conditions

FaDu (hypopharyngeal) and SCC25 (tongue) HNSCC cell lines were obtained from the American Type Culture Collection (ATCC; Manassas, VA, USA). Cells were maintained in Dulbecco's modified Eagle medium/F12 containing 10 % FBS and 1 % penicillin—streptomycin at 37 °C in a humidified 5 % CO_2 atmosphere. Sub-culturing was carried out at 70—80 % confluence using 0.05 % trypsin—EDTA (Gibco, Grand Island, NY, USA).

Genchip analysis

Total RNA was extracted from CAFs and NFs with the RNeasy Mini Kit (Qiagen, Valencia, CA, USA) and its integrity assessed on an Agilent 2100 Bioanalyzer (Agilent

Technologies, Santa Clara, CA, USA). cDNA synthesis, labelling, and hybridisation were performed on the GeneChip™ Human Genome U133 Plus 2.0 Array (Affymetrix, Santa Clara, CA, USA) following the manufacturer's protocol. Arrays were processed on an Affymetrix Fluidics Station and scanned with a GeneChip™ Scanner 3000. Data normalisation and statistical analysis were undertaken in GeneSpring GX (Agilent Technologies). Genes exhibiting > 2-fold change with $P < 0.05$ were deemed differentially expressed.

Quantitative real-time PCR (qPCR)

Total RNA was isolated from cultured fibroblasts and HNSCC cell lines with TRIzol reagent (Invitrogen, Waltham, MA, USA) or an equivalent extraction kit, following the manufacturer's instructions. One microgram of RNA was reverse-transcribed to first-strand cDNA using the High-Capacity cDNA Reverse Transcription Kit (Applied Biosystems, Waltham, MA, USA). qPCR reactions were prepared with SYBR™ Green PCR Master Mix (Applied Biosystems) and run on an ABI 7500 Fast Real-Time PCR System. The following primers were used in Table S1. Thermocycling conditions were 95 °C for 2 min, followed by 40 cycles of 95 °C for 10 s and 60 °C for 30 s. Relative gene expression was determined by the 2^(−ΔΔCt) method, normalizing each target gene to GAPDH.

Western blotting

CAFs, NFs, FaDu and SCC25 cells were lysed in RIPA buffer (50 mM Tris—HCl, pH 7.4; 150 mM NaCl; 1 % NP-40; 0.25 % sodium deoxycholate) with protease/phosphatase inhibitors. Protein concentration was determined by BCA. Equal amounts (20—40 μg) were resolved on 8—12 % SDS—PAGE and transferred to PVDF membranes. Membranes were blocked for 1 h at room temperature in 5 % non-fat milk/TBS-T (20 mM Tris, 150 mM NaCl, 0.1 % Tween-20) and incubated overnight at 4 °C with primary antibodies are listed in Table S2. After TBS-T washes, blots were incubated with HRP-conjugated secondary antibodies for 1 h. Signals were developed by enhanced chemiluminescence and captured on film or a CCD imager. Band intensities were quantified in ImageJ and normalised to beta-tubulin.

Enzyme-linked immunosorbent assay for IL-32

Conditioned media from CAFs and NFs were collected after 24—48 h in serum-free DMEM/F12, centrifuged at 1 000×*g* for 5 min to remove debris, and stored at −80 °C. IL-32 concentration was measured with a human IL-32 ELISA kit (Millipore) following the supplier's protocol. Samples and standards were added to 96-well plates pre-coated with anti-IL-32 capture antibodies, followed by biotinylated detection antibody and streptavidin—HRP. Absorbance at 450 nm was recorded on a microplate reader, and concentrations were extrapolated from a standard curve generated with recombinant IL-32.

Migration and invasion assays

Cell motility was assessed in Transwell chambers with 8 μm-pore polycarbonate membranes (Corning, NY, USA). FaDu

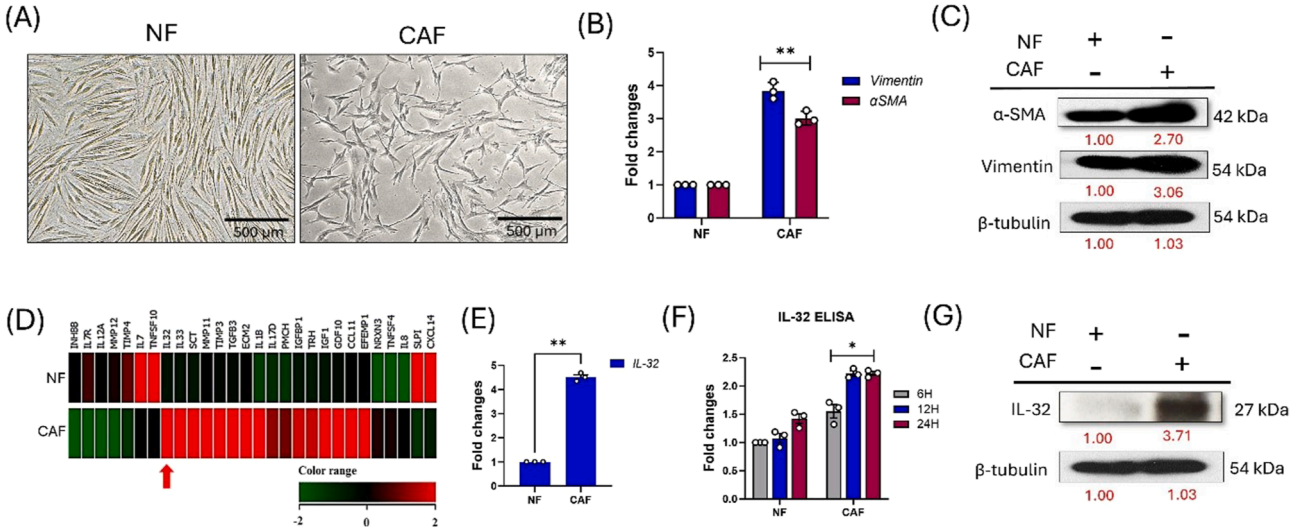

Figure 1 Cancer-associated fibroblasts (CAFs) over-express interleukin-32 (IL-32) relative to normal fibroblasts (NFs). Phase-contrast micrographs showing the spindle-shaped morphology of NFs and the larger, irregular polygonal appearance of CAFs. Scale bars = 500 μm (A). Quantitative real-time PCR analysis of α-smooth-muscle actin (α-SMA) and vimentin transcripts; data are mean ± SD (n = 3), $^{**}P < 0.001$ versus NF (B). Immunoblotting of α-SMA and vimentin in NFs and CAFs; β-tubulin serves as a loading control (C). Heat-map of cytokine-related genes from cDNA microarray profiling (green = down-regulation, red = up-regulation). The red arrow highlights IL-32, which shows > 2-fold up-regulation in CAFs (D). qPCR validation of IL-32 mRNA expression; mean ± SD (n = 3), $^{**}P < 0.001$ versus NF (E). ELISA quantification of secreted IL-32 in conditioned medium collected at 6, 12 and 24 h; mean ± SD (n = 3), $^{*}P < 0.05$ versus NF at the corresponding time-point (F). Immunoblot of cellular IL-32 protein; β-tubulin is the loading control and red numbers indicate relative band intensity normalised to NF. Together, these data confirm that CAFs are a major source of IL-32 within the HNSCC tumour microenvironment (G).

and SCC25 cells pre-treated with CAF-CM or recombinant IL-32 (rIL-32; 50 ng mL^{-1}) were seeded (1×10^5 cells) in serum-free medium into the upper chamber. For invasion assays, inserts were pre-coated with Matrigel diluted 1:5 in serum-free medium; 2×10^5 cells were used and incubated for 24—48 h. The lower chamber contained complete medium. Non-migratory cells were removed; membranes fixed in 4 % paraformaldehyde, stained with 0.1 % crystal violet, underside cells counted in five fields. Results are expressed as mean ± SD (n = 3).

Three-dimensional organotypic culture

A collagen-I/Matrigel mixture (1:1; final collagen concentration 2 mg mL^{-1}) containing 5×10^6 CAFs was dispensed into 12 mm cell-culture inserts (Millipore) and allowed to polymerise for 1 h at 37 °C. HNSCC cells (2×10^5) were then seeded on the gel surface. Cultures were maintained at an air—liquid interface, with medium changed every 2—3 d. After 14 d, gels were fixed in 10 % neutral-buffered formalin, paraffin-embedded, and sectioned at 4 μm. Sections were stained with haematoxylin and eosin (H&E) and examined under a bright-field microscope (Leica Microsystems, Wetzlar, Germany). Invasion depth was quantified in ImageJ.

Flow cytometry for CSC markers

Cells were harvested, washed in PBS, and incubated for 30 min at 4 °C with fluorochrome-conjugated antibodies against CD24 (PE), CD44 (FITC), and CD133 (FITC) (BD Biosciences, USA). After washing, fluorescence was analysed on a flow cytometer, and data processed with FlowJo (Ashland, OR, USA). Results represent mean ± SD of three independent experiments.

Immunohistochemistry (IHC) and scoring

FFPE HNSCC (n = 35) 4-μm sections were deparaffinised, rehydrated, and retrieved (10 mM citrate, pH 6.0, 20 min). After blocking (3 % H_2O_2; 5 % serum), sections were incubated overnight at 4 °C with anti-IL-32 (Abcam), detected by HRP—DAB, counterstained with haematoxylin. Two

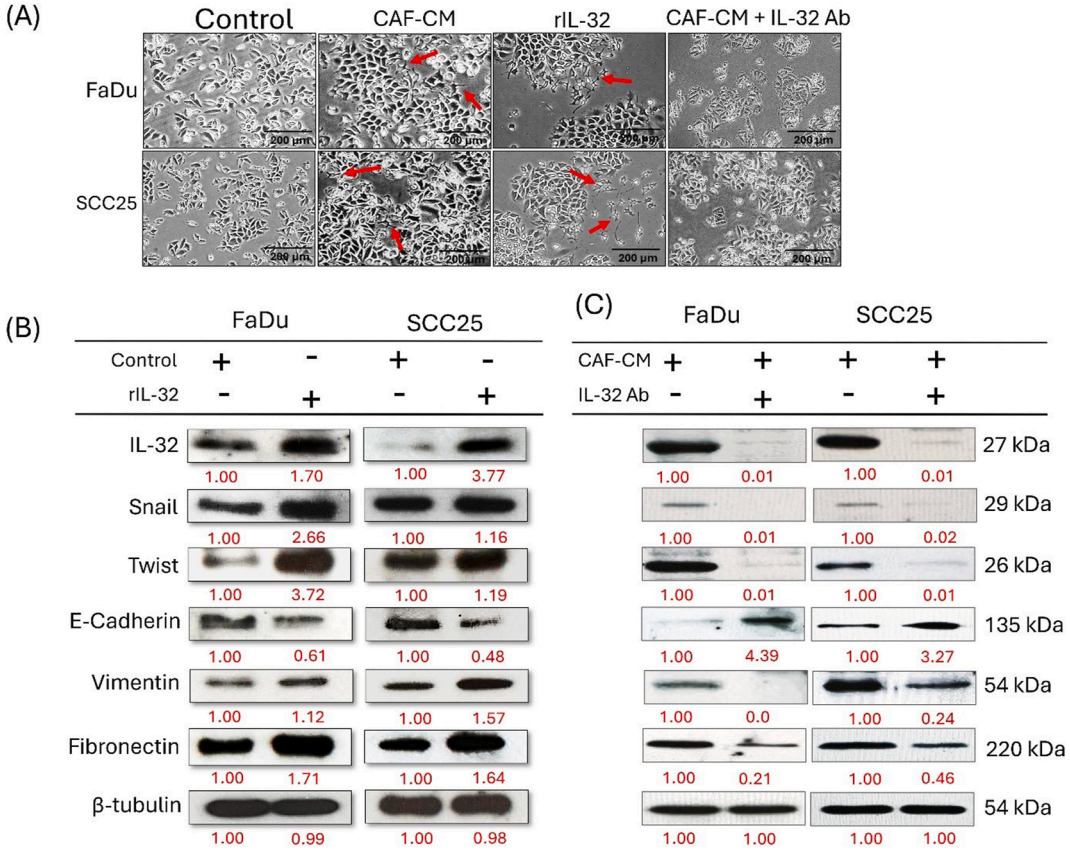

Figure 2 Interleukin-32 (IL-32) induces EMT in HNSCC cells, and neutralisation of IL-32 attenuates EMT-associated morphology and proteins. Phase-contrast images of FaDu and SCC25 cells cultured for 24 h in control medium, CAF-conditioned medium (CAF-CM), recombinant IL-32 (rIL-32, 50 ng mL^{-1}), or CAF-CM plus an IL-32-neutralising antibody (IL-32 Ab). CAF-CM and rIL-32 induce elongated, spindle-like morphology with microspike-like protrusions (red arrows), whereas addition of IL-32 Ab markedly suppresses these features. Scale bars = 200 μm (A). Immunoblots showing EMT-related protein changes in FaDu and SCC25 cells with or without rIL-32. rIL-32 increases IL-32, Snail, Twist, Vimentin and Fibronectin, while reducing the epithelial marker E-cadherin. β-Tubulin serves as the loading control (B). Western-blot comparison of CAF-CM versus CAF-CM + IL-32 Ab. Neutralising IL-32 diminishes IL-32, Snail and Twist, restores E-cadherin, and lowers Vimentin and Fibronectin levels (C). Together these data confirm that IL-32 is sufficient to trigger EMT in head and neck squamous cell carcinoma cells.

blinded observers scored tumour cells and fibroblasts for intensity 0–3+ and % area; data were dichotomised for analysis as Low (0/1+) vs High (2/3+); discrepancies were resolved by consensus.

Statistical analysis

All experiments were performed at least in triplicate. Data are presented as mean ± standard deviation (SD). Two-group comparisons employed the two-tailed Student's *t*-test, while multiple comparisons used one-way ANOVA with Tukey's post-hoc test. A *P*-value <0.05 was considered statistically significant. Analyses were conducted in GraphPad Prism (version X; GraphPad Prism, San Diego,CA, USA) or SPSS Statistics (IBM, Armonk, NY, USA).

Results

cDNA microarray identifies IL-32 as markedly up-regulated in CAFs

Morphologically, normal fibroblasts (NFs) displayed a uniform spindle-shaped appearance, whereas cancer-

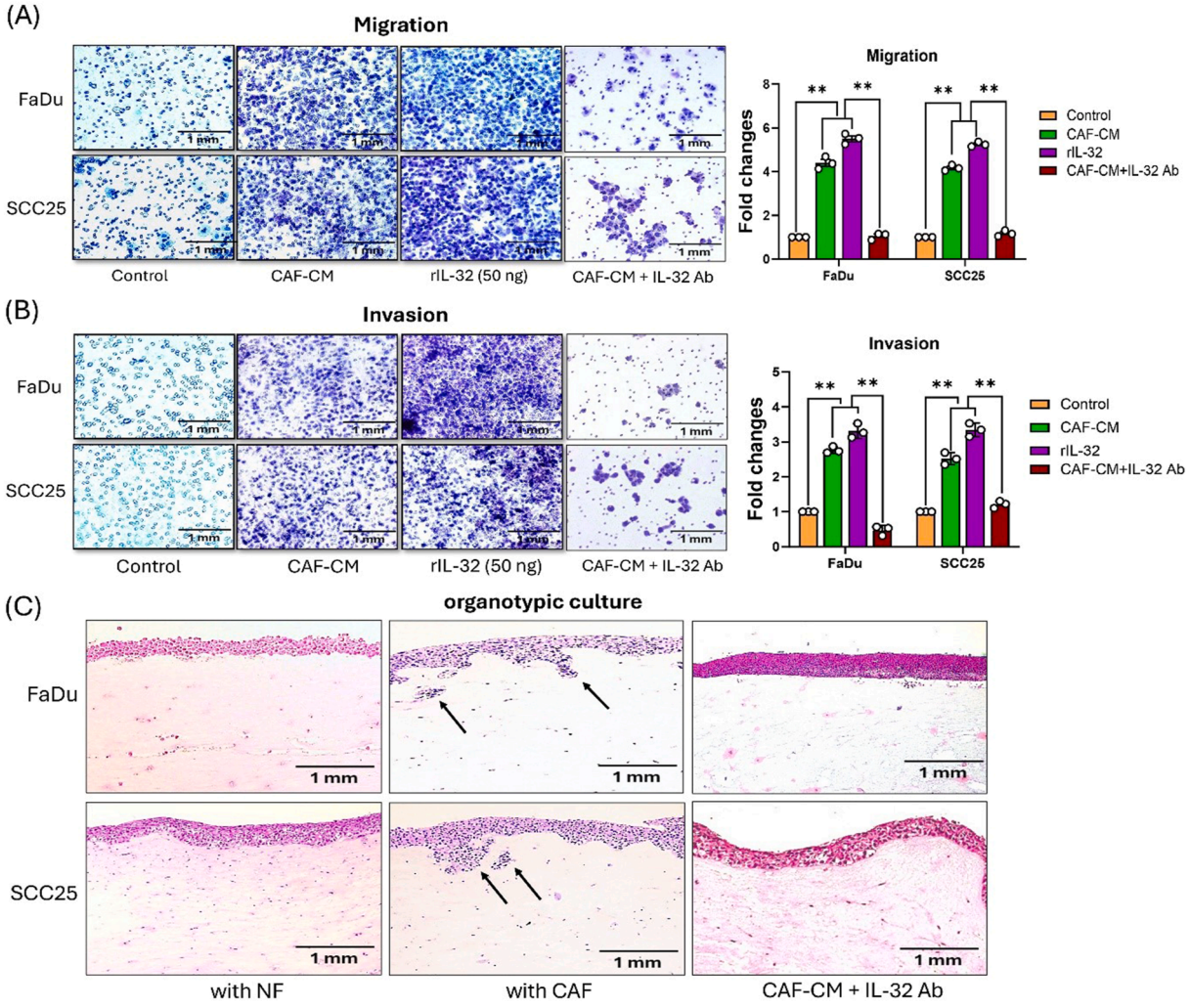

Figure 3 CAF-derived interleukin-32 (IL-32) promotes migration and invasion of HNSCC cells, and IL-32 neutralisation reverses these effects. Migration assay. Crystal-violet-stained FaDu and SCC25 cells that traversed 8 μm Transwell filters after 24 h in control medium, CAF-CM or recombinant IL-32 (50 ng mL^{-1}) or CAF-CM plus an IL-32-neutralising antibody (CAF-CM + IL-32 Ab). CAF-CM and rIL-32 markedly increased motility, whereas addition of IL-32 Ab reduced migration towards near-baseline levels. Right, quantification as fold change relative to control (mean ± SD, n = 3; one-way ANOVA with Tukey's post-hoc; $^{**}P < 0.01$ vs control). Scale bars = 1 mm (A). Invasion assay. Cells were seeded on Matrigel-coated inserts and allowed to invade for 48 h under the same conditions. Quantification (right) indicates a significant 1.5- to 2-fold increase in invading cells with CAF-CM or rIL-32, while IL-32 Ab blunted this effect (mean ± SD, n = 3; $^{**}P < 0.01$ vs control). Scale bars = 1 mm (B). Three-dimensional organotypic model. Haematoxylin-and-eosin-stained sections of collagen/Matrigel gels populated with normal fibroblasts (NF) or CAFs and overlaid with FaDu or SCC25 cells. After 14 d, CAF co-culture produced deeper epithelial invasion (arrows) compared with NF controls, whereas inclusion of IL-32 Ab with CAF-CM largely abolished invasion. Scale bars = 1 mm (C). Collectively, these data confirm that CAF-secreted IL-32 potentiates HNSCC cell migration and invasion in both 2-D and physiologically relevant 3-D settings.

associated fibroblasts (CAFs) were larger, irregular, and polygonal (Fig. 1A). Quantitative real-time PCR (qPCR) (Fig. 1B) and Western blotting (Fig. 1C) confirmed significantly higher expression of α-smooth-muscle actin (α-SMA) and vimentin in CAFs, consistent with their activated phenotype. Global gene-expression profiling by cDNA microarray revealed a > 2-fold increase in IL-32 transcripts in CAFs relative to NFs (Fig. 1D). These findings were validated by qPCR (Fig. 1E), ELISA (Fig. 1F), and Western blotting (Fig. 1G), all of which showed significantly greater IL-32 mRNA and protein levels in CAFs ($P < 0.001$ and $P < 0.05$). CAF-conditioned medium contained two-to three-fold more secreted IL-32 than NF medium, indicating that CAFs are a major source of this pro-inflammatory cytokine in the HNSCC tumour micro-environment.

IL-32 drives epithelial–mesenchymal transition in HNSCC cells

FaDu and SCC25 cells exposed to CAF-conditioned medium (CAF-CM) or recombinant IL-32 (rIL-32) adopted an elongated, spindle-like morphology characteristic of epithelial–mesenchymal transition (EMT), whereas control cells retained a cobblestone epithelial appearance (Fig. 2A). Importantly, addition of an IL-32-neutralising antibody to CAF-CM largely abolished these morphological changes (Fig. 2A). Western blotting confirmed marked down-regulation of the epithelial marker E-cadherin and concomitant up-regulation of mesenchymal markers Vimentin, Fibronectin, Snail, and Twist in treated cells (Fig. 2B), while IL-32 neutralisation in CAF-CM restored E-

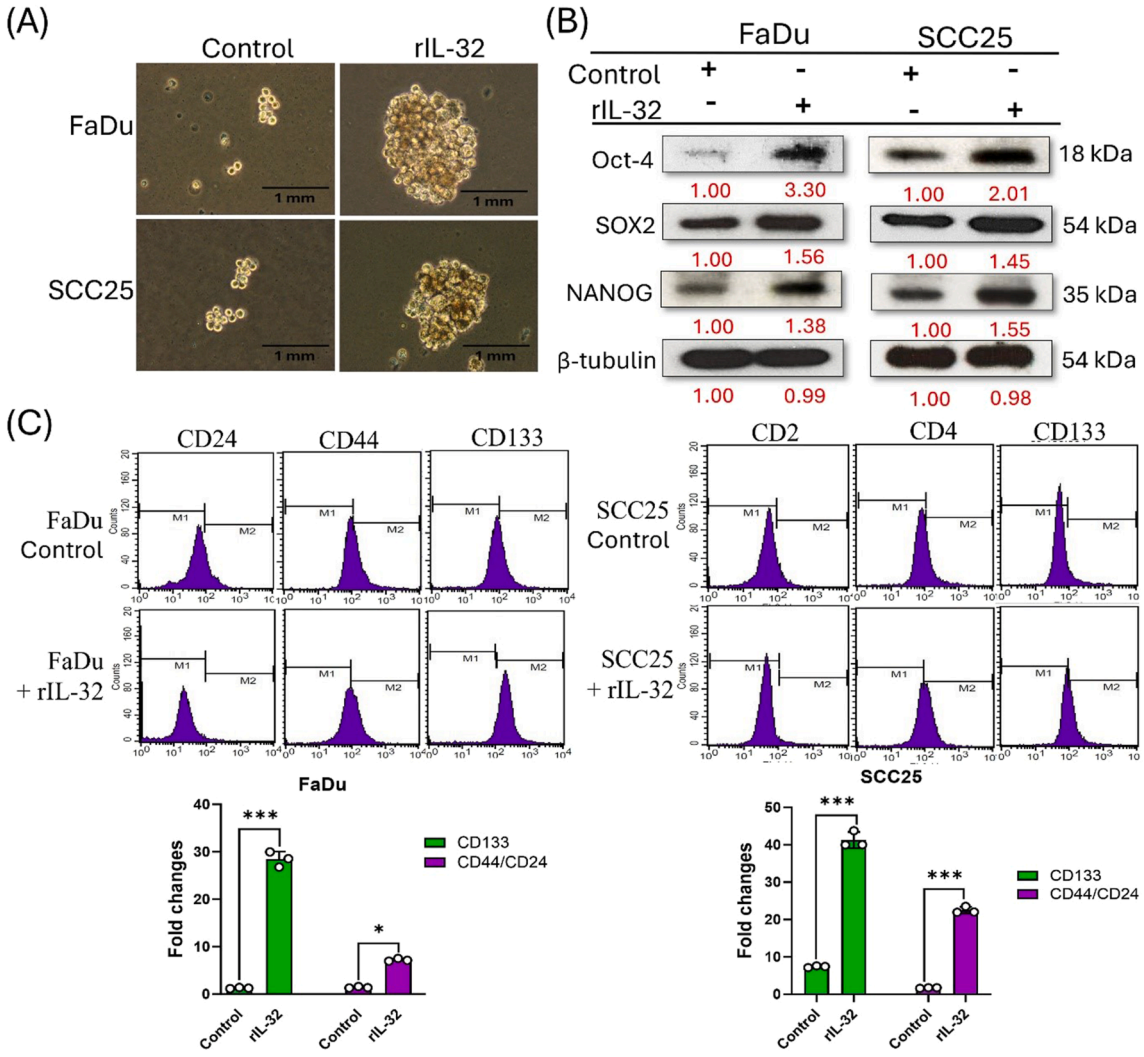

Figure 4 Interleukin-32 (IL-32) enhances cancer-stem-cell (CSC) properties in HNSCC cells. Representative phase-contrast micrographs of tumourspheres formed by FaDu and SCC25 cells cultured for 10 days in serum-free medium with or without recombinant IL-32 (rIL-32, 50 ng mL^{-1}). rIL-32 treatment markedly increases both sphere size and number. Scale bars = 1 mm (A). Immunoblots showing stemness-associated transcription factors Oct-4, SOX2 and NANOG in control (WT) and rIL-32-treated cells. β-Tubulin serves as a loading control; rIL-32 elevates all three markers, indicating augmented stemness (B). Flow-cytometric analysis of surface CSC markers. Histograms illustrate CD24, CD44 and CD133 expression profiles for WT and rIL-32-treated FaDu (left) and SCC25 (right) populations; M2 gates (purple) represent positive cells. Bar graphs (bottom) depict mean ± SD fold change in $CD44^+/CD24^+$ and $CD133^+$ subsets (n = 3). *$P < 0.05$; ***$P < 0.001$ versus control (two-tailed t-test). These data demonstrate that IL-32 not only drives EMT and invasion but also potentiates CSC traits in head and neck squamous cell carcinoma cells (C).

cadherin and lowered Snail, Twist, Vimentin and Fibronectin relative to CAF-CM alone (Fig. 2C). Collectively, these data indicate that IL-32 is sufficient to trigger EMT and is a key mediator of CAF-driven EMT in HNSCC.

CAF-derived IL-32 enhances HNSCC cell migration and invasion

Transwell assays showed that CAF-CM or rIL-32 (50 ng mL^{-1}) significantly increased the migratory and invasive capacities of FaDu and SCC25 cells compared with controls (1.5–2.0-fold; $P < 0.01$) Addition of an IL-32-neutralising antibody to CAF-CM (CAF-CM + IL-32 Ab) markedly blunted these effects, reducing migrated and invaded cell numbers towards baseline and significantly lower than CAF-CM alone ($P < 0.05$) (Fig. 3A and B). In collagen/Matrigel cultures, co-culture with CAFs or rIL-32 treatment drove substantially deeper epithelial invasion over 14 days compared with NF controls ($P < 0.05$), whereas inclusion of IL-32 Ab with CAF-CM largely abolished the invasive front, confirming that CAF-secreted IL-32 is a key mediator of HNSCC invasion in a physiologically relevant setting.

IL-32 augments cancer-stem-cell properties

Sphere-formation assays revealed that rIL-32 significantly increased both the size and number of tumourspheres generated by FaDu and SCC25 cells (Fig. 4A). Western blot analysis demonstrated elevated expression of stemness factors OCT4, SOX2, and Nanog in IL-32-treated cells (Fig. 4B). Flow-cytometric profiling showed higher proportions of $CD24^{+}$, $CD44^{+}$, and $CD133^{+}$ sub-populations following IL-32 exposure (Fig. 4C). Collectively, these results indicate that IL-32 not only promotes EMT and invasion but also endows HNSCC cells with enhanced cancer-stem-cell characteristics, thereby contributing to tumour aggressiveness and potential recurrence.

IL-32 is highly expressed in HNSCC tissues and associates with poorer survival

Immunohistochemistry showed cytoplasmic IL-32 staining in tumour nests and CAF-rich stroma. Cases were stratified by intensity as Negative, Low (1+), or High (2+/3+): 3/35 (8.6 %) Negative, 11/35 (31.4 %) Low, and 21/35 (60.0 %) High (Fig. 5A). For analyses, specimens were dichotomised into Low (0/1+) versus High (2/3+). Kaplan–Meier curves demonstrated significantly poorer overall survival for the High IL-32 group compared with the Low group (log-rank $P = 0.025$; Fig. 5B). These clinicopathological data align with our in-vitro findings and support IL-32 as a marker of aggressive disease biology in HNSCC.

Discussion

Our data demonstrate that cancer-associated fibroblasts (CAFs) are a dominant stromal source of interleukin-32 (IL-32) in HNSCC and that IL-32 is a key effector of malignant progression. CAFs showed an activated phenotype (α-SMA/vimentin),[18] and cDNA microarray/qPCR/ELISA/Western blot confirmed marked IL-32 up-regulation and secretion. Functionally, CAF-CM or rIL-32 induced a classic EMT phenotype in FaDu and SCC25 cells—spindle-like morphology with microspikes, loss of E-cadherin, and gains in vimentin, fibronectin, Snail and Twist.[19]

These effects were attenuated by an IL-32-neutralising antibody, which restored epithelial features and reduced EMT markers. Consistently, migration, invasion and three-dimensional organotypic assays showed that IL-32 drives motility and matrix penetration, whereas IL-32 blockade

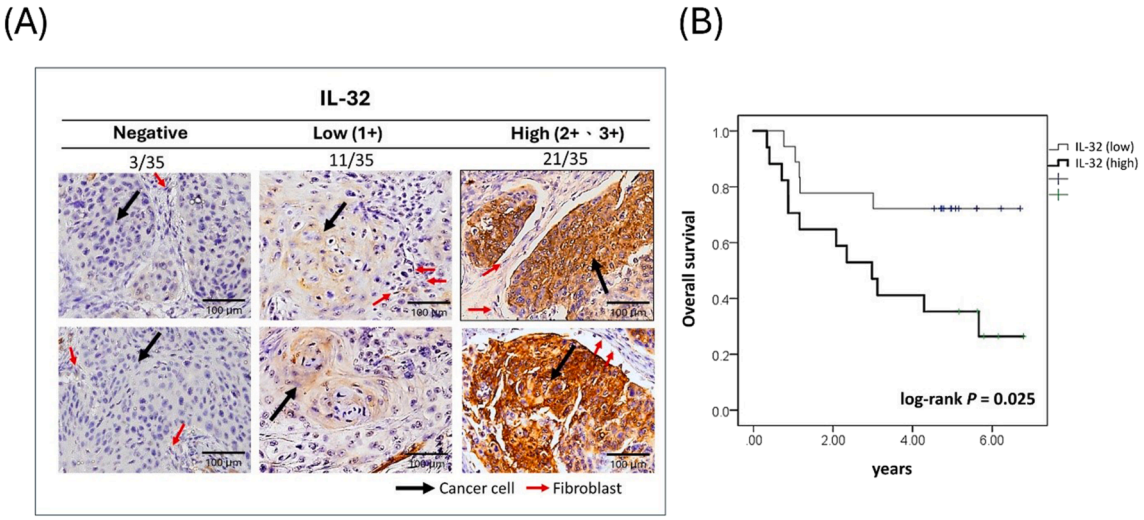

Figure 5 Clinicopathological relevance of interleukin-32 (IL-32) in HNSCC tissues. Representative immunohistochemistry (IHC) for IL-32 in human HNSCC sections stratified by staining intensity: Negative, Low (1+), and High (2+/3+). Fractions above panels indicate case numbers in each category (negative 3/35, low 11/35, high 21/35). Brown chromogen (DAB) marks IL-32-positive cells with haematoxylin counterstain. Black arrows denote tumour cells; red arrows indicate stromal fibroblasts. Scale bars as indicated (A). Kaplan–Meier analysis of overall survival for patients grouped by IL-32 expression (High: 2+/3+; Low: 0/1+). High IL-32 expression is associated with poorer survival (log-rank $P = 0.025$) (B).

blunted these behaviours. IL-32 also strengthened cancer-stem-cell traits,[20] increased sphere-forming efficiency, elevated core stemness transcription factors (OCT4, SOX2, Nanog),[21,22] and expanded $CD24^+$, $CD44^+$, and $CD133^+$ subpopulations.[23–25] Finally, tissue immunohistochemistry linked high IL-32 expression to poorer overall survival, underscoring clinical relevance. The enrichment of CSC traits is clinically pertinent, as CSCs drive recurrence, metastatic spread, and resistance to conventional therapies.[26]

These mechanistic insights complement clinical evidence that *Fusobacterium nucleatum* and IL-32 co-predict nodal metastasis pre-operatively in head and neck cancer; whereas that study positions IL-32 as a predictive biomarker, we delineate how CAF-derived IL-32 drives invasion and dissemination through EMT and stemness programmes, implicating a convergent dysbiosis—inflammation—stromal IL-32 axis in metastatic risk.[17]

Our data indicate that IL-32 is enriched in cancer-associated fibroblasts and, under experimental conditions, is associated with EMT-like changes, increased motility and invasion, and stemness-related features in HNSCC cells; these effects were attenuated by IL-32 neutralisation. In tissue samples, higher IL-32 expression was associated with poorer survival in this cohort. While supportive of a role for IL-32 within the tumour—stroma axis, these findings should be interpreted cautiously and validated *in vivo* before any clinical application is considered. If corroborated, IL-32 may warrant evaluation as a biomarker and a potential stromal-directed target, including in combination with anti-EMT and anti-CSC approaches.

Declaration of competing interest

The authors have no conflicts of interest relevant to this article.

Acknowledgments

The study was funded by the Tri-Service General Hospital (Grant No. TSGH_E113245). Experiments and data analysis were partly performed using the National Defense Medical University (Taipei, Taiwan). We would like to thank Si-Chan Huang for his technical support throughout the course of this study.

Appendix A. Supplementary data

Supplementary data to this article can be found online at https://doi.org/10.1016/j.jds.2025.10.010.

References

1. Barsouk A, Aluru JS, Rawla P, et al. Epidemiology, risk factors, and prevention of head and neck squamous cell carcinoma. *Med Sci* 2023;11:42.
2. Sung H, Ferlay J, Siegel RL, et al. Global cancer statistics 2020: GLOBOCAN estimates of incidence and mortality worldwide for 36 cancers in 185 countries. *CA Cancer J Clin* 2021;71:209—49.
3. Cao W, Qin K, Li F, et al. Comparative study of cancer profiles between 2020 and 2022 using global cancer statistics (GLOBOCAN). *J Natl Cancer Cent* 2024;4:128—34.
4. Rumgay H, Nethan ST, Shah R, et al. Global burden of oral cancer in 2022 attributable to smokeless tobacco and areca nut consumption: a population attributable fraction analysis. *Lancet Oncol* 2024;25:1413—23.
5. Smith CDL, McMahon AD, Purkayastha M, et al. Head and neck cancer incidence is rising but the sociodemographic profile is unchanging: a population epidemiological study (2001-2020). *BJC Rep* 2024;2:71.
6. Xie Y, Wang X, Wang W, et al. Epithelial-mesenchymal transition orchestrates tumor microenvironment: current perceptions and challenges. *J Transl Med* 2025;23:386.
7. Wright K, Ly T, Kriet M, et al. Cancer-associated fibroblasts: master tumor microenvironment modifiers. *Cancers (Basel)* 2023;15:1899.
8. Li X, Escoffier H, Sauter T, et al. Targeting fibroblast-derived interleukin 6: a strategy to overcome epithelial-mesenchymal transition and radioresistance in head and neck cancer. *Cancers (Basel)* 2025;17:267.
9. Mao H, Zhao X, Sun SC. NF-kappaB in inflammation and cancer. *Cell Mol Immunol* 2025;22:811—39.
10. Staal J, Beyaert R. Inflammation and NF-kappaB signaling in prostate cancer: mechanisms and clinical implications. *Cells* 2018;7:122.
11. Xie Y, Liu F, Wu Y, et al. Inflammation in cancer: therapeutic opportunities from new insights. *Mol Cancer* 2025;24:51.
12. Pal A, Barrett TF, Paolini R, et al. Partial EMT in head and neck cancer biology: a spectrum instead of a switch. *Oncogene* 2021;40:5049—65.
13. Li K, Zeng X, Liu P, et al. The role of inflammation-associated factors in head and neck squamous cell carcinoma. *J Inflamm Res* 2023;16:4301—15.
14. Meng D, Dong H, Wang C, et al. Role of interleukin-32 in cancer progression. *Oncol Lett* 2024;27:54.
15. Shim S, Lee S, Hisham Y, et al. A paradoxical effect of interleukin-32 isoforms on cancer. *Front Immunol* 2022;13:837590.
16. Han F, Ma J. Pan-cancer analysis reveals IL32 is a potential prognostic and immunotherapeutic biomarker in cancer. *Sci Rep* 2024;14:8129.
17. Wang Z, Huang H, Yuan X, et al. Fusobacterium nucleatum and IL-32 co-predict nodal metastasis preoperatively in head and neck cancer. *Transl Cancer Res* 2025;14:3359—72.
18. El Herch I, Tornaas S, Dongre HN, et al. Heterogeneity of cancer-associated fibroblasts and tumor-promoting roles in head and neck squamous cell carcinoma. *Front Mol Biosci* 2024;11:1340024.
19. Gong L, Liu G, Zhu H, et al. IL-32 induces epithelial-mesenchymal transition by triggering endoplasmic reticulum stress in A549 cells. *BMC Pulm Med* 2020;20:278.
20. Lee YS, Kim KC, Mongre RK, et al. IL-32gamma suppresses lung cancer stem cell growth via inhibition of ITGAV-mediated STAT5 pathway. *Cell Death Dis* 2019;10:506.
21. Caballero-Borrego M, Grau JJ, Baste N, et al. Cancer stem cell biomarkers in locally advanced head and neck squamous cell carcinoma. *Braz J Otorhinolaryngol* 2025;91:101689.
22. Yu SS, Cirillo N. The molecular markers of cancer stem cells in head and neck tumors. *J Cell Physiol* 2020;235:65—73.
23. Kavitha L, Vijayashree Priyadharsini J, Kattula D, et al. Expression of CD44 in head and neck squamous cell carcinoma-An in-silico study. *Glob Med Genet* 2023;10:221—8.
24. Ghazi N, Saghravanian N, Anvari K, et al. Correlation between clinicopathological indices and expression of cluster of differentiation 24 and cluster of differentiation 44 biomarkers in oral epithelial dysplasia and oral squamous cell carcinoma patients: a follow-up study. *Dent Res J* 2024;21:50.

25. Mannelli G, Magnelli L, Deganello A, et al. Detection of putative stem cell markers, CD44/CD133, in primary and lymph node metastases in head and neck squamous cell carcinomas. A preliminary immunohistochemical and in vitro study. *Clin Otolaryngol* 2015;40:312—20.

26. Manchanda AS, Rai HK, Kaur M, et al. Cancer stem cells targeted therapy: a changing concept in head and neck squamous cell carcinoma. *J Oral Maxillofac Pathol* 2024;28:455—63.